Chemical Process Design Vol.3 No.2 (2024) 61-80

University of Sistan and Baluchestan

Chemical Process Design

Available online at http://cpd.usb.ac.ir/

Innovative Heat Integration using Bottom Flashing Method: Energy, Exergy, Economic, and Environmental Evaluations of Natural Gas Sweetening Process

Nargess Eyvazi-Abhari[1,*], Samira Ahmadi[2], Sayna Rahbari[3], Melika Esperi[4], Fateme Ezati Kamkar[5], Hanieh Asvadi[6]

[1]M.Sc. gradute of chemical engineering at Iran University of Science and Technology, Tehran, Iran
[2]Ph.D. candidate of chemical engineering at Iran University of Science and Technology, Tehran, Iran
[3]Ph.D. student of chemical engineering at Amirkabir University of Technology, Tehran, Iran
[4]M.Sc. graduate of chemical engineering at Sharif University of Technology, Tehran, Iran
[5]M.Sc. graduate of chemical engineering at Amirkabir University of Technology, Tehran, Iran
[6]Ph.D candidate of chemical engineering at Isfahan University of Technology, Isfahan, Iran

ARTICLE INFO

Article history:
Received: 2024-09-10
Received in revised form: 2024-11-02
Accepted: 2024-12-03
Published online: 2024-12-03

Keywords:
Bottom flashing; CO_2 emission; Energy/exergy analysis; Heat integration; Sour gas sweetening; Vapor recompression

DOI: *10.22111/cpd.2025.50477.1045*

ABSTRACT

The process of sour gas sweetening by amine has found extensive applications in the chemical industries. This process is typically associated with significant CO_2 emissions and energy consumption due to the use of absorption and distillation columns. In this regard, the heat integration of the process is essential to reduce the costs and environmental consequences. A heat exchanger is used in most gas refineries between the two columns which can decrease the consumption utility. The energy consumption of the process is still high due to the presence of a reboiler and a condenser in the solvent recovery column. In this research, vapor recompression (VRC) and bottom flashing (BF) were employed for heat integration. To compare the proposed methods with the conventional approaches, four different procedures were accurately simulated and their energy consumption, total annual cost (TAC), exergy efficiency, exergy loss, and CO_2 emissions were compared. The results indicated that BF heat integration outperformed the conventional methods by significantly reducing energy consumption, TAC, exergy loss, and CO_2 emissions, while enhancing exergy efficiency, primarily due to the reduction of the need for hot and cold utilities in the recovery column.

1. Introduction

The global demand for natural gas has recently increased due to its lower carbon dioxide emission compared to other fossil fuels such as crude oil and coal [1]. Most of the natural gas resources are sour, the CO_2 content of about 30% of these resources ranges from 15-80%, suggesting their great sulfur and carbon dioxide contents [2]. This is

Corresponding author. Tel: +989124038058
E-mail address: nargess.eyvazi@gmail.com (N. Eyvazi-Abhari).

specifically true in the Middle East, where 60% of the natural gas resources are sour. The consumption of sour gas is harmful to the environment, necessitating the removal of acidic substances prior to its application [3].

As a fundamental procedure in gas treatment, gas sweetening involves the elimination of acidic compounds such as CO_2 and hydrogen sulfide [4, 5]. Various methods exist for natural gas sweetening, including chemical, physical, biological, ionic, and hybrid solvents for acid gas absorption [3]. Amine-based processes, though widely used due to their high affinity for sour gas components, have high energy consumption, making optimization crucial [6, 7]. Compared to ammonia, carbonates, and amino acid solvents, amines offer benefits like high absorption efficiency and easy reclamation but face challenges such as corrosion, thermal degradation, and high regeneration energy [8, 9]. The energy consumption in amine-assisted gas sweetening has been reduced through novel solvent formulations, process optimization, or equipment modifications [10]. Mono-ethanolamine (MEA) is the most common alkanolamine due to its high reactivity and low cost, but it has been found to suffer from degradation, corrosion, and low selectivity for H_2S [11, 12]. Muchan et al. [13], found that while all tested alkanolamine compositions reduced energy consumption, those with more hydroxyl groups showed weaker CO_2 absorption due to electron withdrawal effects [13]. Ellaf et al. [14], demonstrated that hybrid solvents, particularly sulfolane and mono-diethanolamine (MDEA), significantly decreased energy use and costs by 20 and 93%, respectively, making them an environmentally favorable alternative [14].

In general, systems that involve vapor, such as stripping and rectifying processes, consume a significant amount of energy. Consequently, numerous energy-efficient technologies have been developed. Notably, heat integration methods like multi-effect distillation, distillation based on external heat pumps, heat-integrated distillation column (HIDiC), feed splitting, and other methods like membrane distillation have proven to be successful in reducing energy usage [15, 16]. The use of a heat integration layout has also been shown to reduce energy consumption and costs by altering the process steps [17].

Among heat integration methods, those employing mechanical vapor recompression heat pumps (MVRHP), which include vapor recompression (VRC) and bottom flashing (BF) distillations, are utilized in various industries. In VRC method, the vapor produced at the top of the distillation column is pressurized again and then directed into the reboiler to serve as a heat source. This approach to distillation is noted for its simplicity and ease of application. While BF technique involves reducing the pressure of the liquid collected at the bottom of the distillation column. A portion of this liquid is then heated and turned into vapor by the heat from the top vapor distillate. Afterward, this vapor is pressurized and introduced at the bottom of the stripping section. BF distillation requires operation at significantly elevated pressures [16].

In recent studies, various methods have been investigated to diminish energy usage in the gas-sweetening process. By introducing two flash columns between the absorption and distillation columns in the standard process, Dai et al. [17], were able to reduce the operating cost and the energy consumption by 2.2×109 $kJ.h^{-1}$ [17]. Long and Lee [18], also decreased the energy consumption of the process that removes acidic gas compounds by applying a heat pump system and heat integration to several distillation columns, which resulted in a 62.5% and 45.9% reduction in the reboiler heat duty and the operating cost, respectively [18].

Amri and Zahid [19], proposed an improved layout for the sweetening unit which lowered the energy consumption by 22% by reducing the amine circulation flow. The outcomes also revealed an 18% lower annual cost of the proposed method in comparison with the initial case [19].

Liu et al. [20], considered three processes of traditional MDE, hydrate-based gas separation, and hydrate-based gas separation coupling MDEA to sweeten natural gases with high H_2S and CO_2 contents. Their results indicated an improvement in the separation of sour compounds in addition to lower capital and operation costs due to the reduction of energy consumption of the solvent recovery unit in the coupled process [20]. Song et al. [7], utilized VRC for recovering the lost heat in the condensation part of the recovery column. Their findings showed that the designed process can recover 38.1 MW of the lost heat and reduce the energy consumption to 7.2 MW.

Sahl et al. [21], reduced the energy consumption of the gas sweetening unit in two stages. They first considered different percentages of sulfinol-M and sulfinol-D and indicated that the solution containing 38% sulfinol-M, 40% sulfolane, and 22% water could decrease the heat load of the reboilers. The heat load of the reboilers was decreased by 65% by optimizing the process. Then they presented heat integration layouts such as Absorber intercooling (AI), lean amine stream split flow (LASSF), rich amine stream split flow (RASSF), mechanical vapor recompression, and 11 combinations of them. They calculated the cost of each layout and the results indicated the LASSF+RASSF combination was selected as the optimal layout with the lowest production costs (4.6 million dollars) due to reducing the equipment size such as the heat exchanger [21]. Lian et al. [22], recovered the cold energy of the produced sweet gas by coupling it to the solvent recovery column to decrease the energy consumption. Then, they utilized a combination of heat pump and feed splitting in the distillation. Their results indicated a 30%, 19.3%, and 13.1% reduction in energy consumption, operation cost, and total annual cost (TAC), respectively [22].

Exergy, as a thermodynamic concept, represents the maximum work extractable from a system in equilibrium with the environment. It is a measure of energy efficiency, identifying where and how much potential work is lost due to irreversibilities in a process. Exergy analysis is vital for optimizing resource management and maximizing effective energy use. [23, 24]. Odejobi et al. [25], addressed the exergy analysis of CO_2 absorption from flue gas and showed that the heat exchanger, the cooler of the lean amine flow, the rich amine flow, and the stripper had the highest exergy loss (820516.24MW, 481343.23MW, and 404273.57MW, respectively). They also indicated that heat transfer, mixing, chemical reaction, and friction in the main units can result in exergy loss [25].

Atsonios et al. [26], considered amine scrubbing, calcium looping (CaL), and air separation unit configurations to absorb CO_2 from gas, flue gas, and air, respectively, considering exergy analysis. According to their results, 7.7% and 1% of the input exergy are lost in the absorption and CO_2 compression units in the amine scrubbing process, respectively. Moreover, in the absorption of CO_2 with MEA solvent, a high MEA/CO_2 ratio and high MEA concentration in the lean solvent can increase the efficacy of the process [26].

Feyzi et al. [27], conducted exergy analysis of the CO_2 absorption process. They enhanced the piperazine content in the solution to decline exergy loss. Their results indicated a decrease in the total exergy loss from 3.25 to 2.63 MW. In other words, a 27% decrease in the molar flow of amine reduced the exergy loss, energy consumption, and service costs by 19, 18, and 25%, respectively [27].

Since the industrial revolution, CO_2 emissions from gas refineries have become a significant environmental concern due to the substantial energy required and the resulting high combustion of fossil fuels. Consequently, reducing CO_2

emissions is a critical consideration in the design of chemical processes [28, 29]. Kangrui Nie et al. [30], applied high gravity technology to CO_2 capture processes with MEA solvents, enhancing energy efficiency and CO_2 emission reduction. This method also improved the absorption rate, equipment size, and mass transfer efficiency compared to traditional processes at normal gravity [30].

This study aims to present an efficient heat integration method to decrease the energy consumption of the amine gas sweetening, to this end, VRC and BF methods were employed for heat integration, no study has so far addressed the use of BF method for sweetening the natural gas with amine. Economic, thermodynamic, and environmental analyses were considered to compare the efficiency of the mentioned methods with conventional approaches in the gas refineries. To this end, the two mentioned methods, along with the two common methods, were rigorously simulated and their energy consumption, TAC, exergy loss, exergy efficiency, and CO_2 emissions were compared.

2. Case study

The present research explored the process of natural gas sweetening by MEA solvent. When the sour gas and the solvent enter the first column, CO_2 and H_2S are separated from the sour gas, and the sweetened gas exits from the top of the first column. The solvent is recovered in the second column and then returns to the first column. Table 1 depicts the feed conditions of the sour gas and the solvent.

Table 1. Inlet conditions of the sour gas and the solvent feeds [31]

Feed characteristic		Sour gas	Solvent (MEA)
Temperature (˚C)		30	30
Pressure (kPa)		3000	5000
Molar flow (kmol.h^{-1})		3888	4377
Mole fraction	Methane	0.85	0
	Ethane	0.04	0
	Propane	0.02	0
	i-butane	0.007	0
	n-butane	0.006	0
	i-pentane	0.004	0
	n-pentane	0.003	0
	Carbon dioxide	0.03	0
	Hydrogen sulfide	0.02	0
	Nitrogen	0.01	0
	Water	0.01	0.8878
	MEA	0	0.1122

3. Methodology

Four arrangements of conventional process (CP), heat-integrated process (HIP), VRC, and BF were first simulated and their total energy consumption, TAC, exergy loss, and exergy efficiency were compared. The applied methods and equations will be discussed in this section.

Aspen HYSYS V.11 was employed to simulate the processes. The Acid Gas-Chemical Solvents thermodynamic package was selected, as it is specifically designed for modeling amine-based solvents, including MEA. This package provides reliable predictions of phase behavior and separation performance, making it suitable for absorption and solvent recovery simulations. The columns were rigorously solved using the Modified HYSIM Inside-Out solution method, rather than shortcut approaches.

3.1. Heat integration

In this paper, VRC and BF methods were used for heat integration of the recovery column.

3.1.1. VRC method

VRC is one of the approaches for the reduction of energy consumption in the distillation column. In this method, the column temperature rises by enhancing the output vapor pressure, enabling heat exchange from the output vapor at the top to the output liquid at the bottom. Consequently, this process declines the consumption of hot and cold utilities. In the VRC method, the vapor leaving the top of the column is transmitted to a compressor where its temperature and pressure increase. It can heat up the flow exiting the bottom of the column by providing a heat exchanger. Afterwards, the pressure of the cooled flow decreases by using a throttling valve before it splits into the top product and some return flow back to the column as the reflux flow. The hot flow leaving the heat exchanger is also divided into the bottom product and some return flow back to the column as the boil-up flow (see Fig. 1).

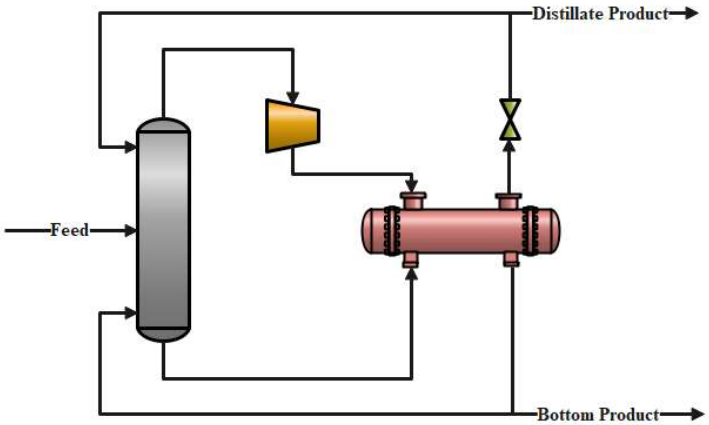

Fig. 1. Schematic representation of the VRC configuration

3.1.2. BF method

BF is another method for heat integration in the distillation columns. In this process, the temperature of the flow exiting the bottom of the column is declined by decreasing its pressure, enabling heat exchange from the vapor leaving the top of the column to the flow exiting the bottom of the column. Therefore, this procedure decreases the consumption of the hot and cold utilities.

In the BF method, the flow leaving the bottom of the column is transmitted to a throttling valve where its temperature and pressure are reduced. Then, the flow is guided to a heat exchanger where it is heated up by the heat from the column's top outflow. The hot flow exiting the heat exchanger is partially separated into the bottom flow and a part that enters the compressor before being sent back to the column as the boil-up flow. The cold outflow of the heat exchanger is separated into the top product and a part returning to the column as the reflux flow (see Fig. 2).

3.2. Calculation of total energy consumption

This section discusses the estimation of total energy consumption for the four mentioned methods. In these processes, the pump and compressor are electricity consumers while the reboiler and condenser supply the required heat of the

process through hot and cold utilities. As the electricity consumption of the pump is much lower than the compressor, it was neglected in the estimation of the total energy consumption.

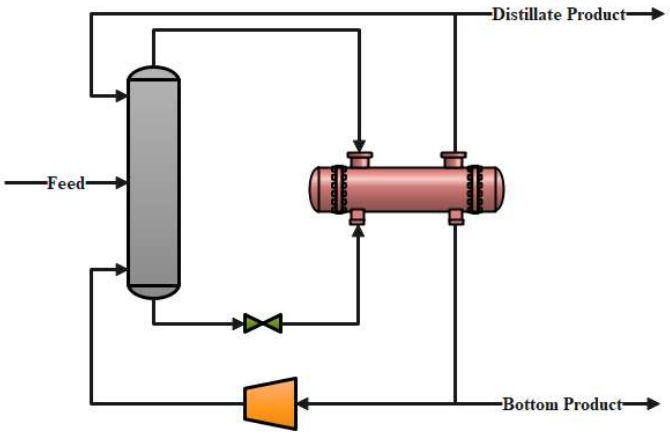

Fig. 2. Schematic representation of the BF configuration

Eq. (1) is utilized to determine the energy of a process without compressor. Each of the VRC and BF methods has a compressor that consumes energy; hence, Eq. (2) is used there instead.

$$Q = Q_r + Q_c \tag{1}$$

$$Q^{'} = Q_r + Q_c + 3W_{Comp} \tag{2}$$

Q and Q' represent the total energy consumption of the process, while Q_c denotes the cold utility, Q_r is the hot utility, and W_{comp} represents the compressor consumption. The compressor efficiency is considered to be 33%, therefore, factor 3 can be applied to convert the electricity energy of the compressor to heat energy [32].

3.3. TAC calculation

Based on Eq. (3), TAC can be regarded as the sum of operating costs and annualized capital expenses. Thus, both operating and capital expenses (C_{Op} and C_{Cap}) can affect the value of TAC. In Eqs. (4) & (5), the effective factors on C_{Op} and C_{Cap} are specified.

$$TAC = f(C_{Op}, C_{Cap}) = C_{Op} + \frac{C_{Cap}}{Payback\ Factor} \tag{3}$$

$$C_{Op} = f(C_{Utility}, T_{cond}, Q_{cond}, T_{reb}, Q_{reb}, C_{elect}) \tag{4}$$

$$C_{Cap} = f(P, H_{Col}, D_{Col}, A_{HX}, C_{pump}, C_{compressor}) \tag{5}$$

Economic calculations were conducted based on the equations and costs for capital investment as presented by Sieder et al. [33]. The details of the economic calculations can be found in the appendix.

3.4. Calculations of exergy loss and exergy efficiency

To calculate exergy loss, the exergy of the mass, heat, and work flows were determined based on Eqs. (6-10). The exergy loss of each piece of equipment and the entire system can be then calculated according to Eq. (11).

$$EX_{stream} = EX_k + EX_p + EX_{ph} + EX_{ch} \quad (6)$$

$$EX_Q = Q(1-\frac{T_0}{T}) \quad (7)$$

$$EX_W = W \quad (8)$$

In Eq. (6), EX_{stream}, EX_k, EX_p, EX_{ph}, and EX_{ch} indicate the stream, kinetic, potential, physical, and chemical exergies of the mass flow, respectively. Regarding constant velocity and height in the static simulation, the potential and kinetic exergies can be neglected. Physical and chemical parts of the mass flow exergy are presented in Eqs. (9) and (10). In Eqs. (7) and (8), EX_Q, Q, T_0, T, EX_W, and W are the heat flux exergy [kW], the ambient temperature [K], the output temperature [K], the work exergy [kW], and the power consumption [kW], respectively. All the values of exergies are expressed in [kW].

$$EX_{ph} = (H - H_0) - T_0 \times (S - S_0) \quad (9)$$

$$EX_{ch} \cong \Delta\mu_i \quad (10)$$

In which, EX_{ph}, H, S, H_0, S_0, Ex_{ch}, and $\Delta\mu_i$, respectively denote the physical exergy [kW], flow enthalpy [kW], flow entropy [kW.K^{-1}], flow enthalpy at the environmental condition [kW], flow entropy at the environmental condition [kW.K^{-1}], chemical exergy [kW], and the chemical potential difference of the component i in the input and output flows [kW]. The chemical potential difference shall be considered in the input and output flows of the distillation, absorption, and flash columns. For mixtures, it can be calculated using Eq. (11).

$$\Delta\mu_{mix} = \Delta H_{mixing} + \Delta\bar{G} \quad (11)$$

$$\sum EX_{out} - \sum EX_{in} + EX_2 - EX_1 + I = 0 \Rightarrow I = \sum EX_{in} - \sum EX_{out} + EX_1 - EX_2 \quad (12)$$

In Eq. (11), ΔH_{mixing} represents the heat of dissolution or mixing, and $\Delta\bar{G}$ signifies the change in Gibbs free energy per mole. In Eq. (12), I, $\sum EX_{in}$, $\sum EX_{out}$, EX_1, and EX_2, respectively represent the exergy loss, sum of the input exergies, sum of the output exergies, and exergies of the initial and secondary states of the system. According to the above equations, the exergy loss can be found in Eqs. (13), (14), (15), (16), and (17), respectively for the conventional distillation column, the pump or the compressor, the throttling valve, the heater or the cooler, and the heat exchanger.

$$I = (EX_F + Q_r(1-\frac{T_0}{T_r})) - (EX_D + EX_B + Q_c(1-\frac{T_0}{T_c})) \quad (13)$$

$$I = H_i - H_e + T_0(S_e - S_i) + W \quad (14)$$

$$I = H_i - H_e + T_0(S_e - S_i) \quad (15)$$

$$I = H_i - H_e + T_0(S_e - S_i) + Q(1-\frac{T_0}{T}) \quad (16)$$

$$I = (H_{c,i} + H_{h,i}) - T_0(S_{c,i} + S_{h,i}) - (H_{c,e} + H_{h,e}) + T_0(S_{c,e} + S_{h,e}) \quad (17)$$

In which, EX_F, EX_D, EX_B, T_c, T_r, H_i, S_i, H_e, S_e, W, Q, $H_{c,i}$, $H_{h,i}$, $S_{c,e}$, and $S_{h,e}$, respectively present exergy of the feed of the distillation column, exergy of the distillate product of the column, exergy of the bottom product of the column, the temperature of the distillate product [K], the temperature of the bottom product [K], inlet flow enthalpy [kW], inlet flow entropy [kW.K^{-1}], outlet flow enthalpy [kW], outlet flow entropy [kW.K^{-1}], work of the pump or compressor [kW], heat duty of the cooler or heater (negative for the cooler and positive for the heater) [kW], enthalpy of the cold

and hot flows at the input of the exchanger [kW], and entropy of the cold and hot flows at the output of the exchanger [kW.K^{-1}].

Various equations can be used to determine the exergy efficiency. The output-to-input ratio is one of these methods which has high error [34-37]. For instance, in the throttling valve (opposite to the turbine), the exergy of the fluid is declined but no work is produced; therefore, the exergy efficiency of the throttling valve is always zero. This result is not obtained based on these equations. Thus, Eq. (18) should be used to determine the exergy efficiency. The exergy efficiency can be obtained from the ratio of the useful produced exergy to the consumed exergy.

$$\eta_{ex} = \frac{Useful\ exergy\ produced\ in\ output}{Consumed\ exergy\ in\ input} \tag{18}$$

Accordingly, the exergy efficiency of the compressor or pump is depicted in Eq. (19), while the exergy efficiency of the heat exchanger can be found in Eq. (20).

$$\eta_{ex,c} = \frac{(h_e - h_i) - T_0(s_e - s_i)}{h_i - h_e} \tag{19}$$

$$\eta_{ex,e} = \frac{[(h_e - h_i) - T_0(s_e - s_i)]_{cold\ stream}}{[(h_i - h_e) - T_0(s_i - s_e)]_{hot\ stream}} \tag{20}$$

In which, $\eta_{ex,c}$, $\eta_{ex,e}$, h_e, s_e, h_i, and s_i, respectively denote the exergy efficiency of the pump or the compressor, exergy efficiency of the heat exchanger, molar enthalpy of the outlet flow [kJ.kmol^{-1}], molar entropy of the outlet flow [kJ.kmol^{-1}.K^{-1}], molar enthalpy of the inlet flow [kJ.kmol^{-1}], and molar entropy of the inlet flow [kJ.kmol^{-1}.K^{-1}]. Eq. (20) can be used for the heat exchangers in which the input and output temperatures of the hot and cold fluids are higher than the ambient temperature. Noteworthy, the exergy efficiency for the throttling valve will be zero according to the definition.

3.5. Calculation of CO_2 emissions

Ultimately, the CO_2 emissions of the four processes were determined both thermally and electrically using Eqs. (21-23). For the thermal utilities, which include the cooling water for the condenser/cooler and the steam for the reboiler/heater, the CO_2 emissions from the steam required for the reboiler/heater are significantly higher than those from preparing the cooling water, due to fuel combustion. Consequently, the CO_2 emissions from the condenser or cooler are considered negligible in all processes. The CO_2 emissions for the reboiler/heater are specifically calculated using Eq. (21) [38].

$$CO_2\,|_{emissions,\ thermal} = \frac{Q_{Fuel}}{NHV} \times \frac{C\%}{100} \times \alpha \tag{21}$$

where Q_{Fuel} is the required fuel to provide the needed steam in the reboiler and can be obtained based on the Eq. (22). NHV is the net heating value which is considered as 39771kJ.kg^{-1}, C% represents the carbon content which is considered 86.5% and α, as the CO_2 molar mass ratio, is noted as 3.67 [38].

$$Q_{Fuel} = \frac{Q_{Proc}}{\lambda_{Proc}}(h_{Proc} - 419) \times \frac{T_{FTB} - T_0}{T_{FTB} - T_{Stack}} \tag{22}$$

In which, Q_{Proc} refers to the reboiler heat duty [kJ.h^{-1}]. λ_{Proc} and h_{Proc} represent the latent heat and enthalpy of the low or medium pressure steam (LPS/MPS) in a reboiler [kJ.kg-1]. T_0 is set at 25˚C as the reference temperature, while the flame temperature, (T_{FTB}), is at 1800˚C, and the stack temperature, (T_{Stack}), is maintained at 160˚C. Additionally, the enthalpy of the boiler feed water is given as 419kJ.kg^{-1} when the water is at 100˚C [38]. CO_2 emission rates for electrical equipment, like compressor, can be calculated according to Eq. (23) [38].

$$CO_2\,|_{emissions,\,electrical} = 51.1\ [kg.GJ^{-1}] \times W_{Comp}\ [GJ.h^{-1}] \tag{23}$$

4. Results and discussion

This section explains the simulation procedure of the four mentioned processes and compares their results based on the total energy consumption, TAC, exergy loss, and exergy efficiency.

4.1. Conventional process (CP)

Fig. 3, depicts the simulated CP by amine solvent, in Aspen HYSYS software. In CP, the main feed, i.e., sour gas, enters the absorption column at the bottom while the solvent (MEA) enters the column from the top. The absorption column operates at high pressure to improve the absorption of gas components, and the maximum pressure drop of 100kPa is considered for this column. In this column, the top product is the sweet gas (free of CO_2 and H_2S) while the solvent with the absorbed impurity leaves the bottom of the column. For purification and solvent recovery, the solvent enters the second distillation column (i.e., solvent recovery column) after reaching the proper temperature at 100 ˚C (by using a heat exchanger and hot utility). The solvent recovery column operates at atmospheric pressure where the bottom product leaves the column in the composition the same as the input solvent. This flow after passing the pump and heat exchanger with cold utility reaches the same temperature and pressure of the input solvent of the absorption column and can be sent back to the absorption column. Since approximately 99.99% of the solvent is recovered and returned to the absorption column, no makeup stream is considered for the input solvent in any of the simulated processes, including CP. The simulation specifications of the CP can be found in Table 2.

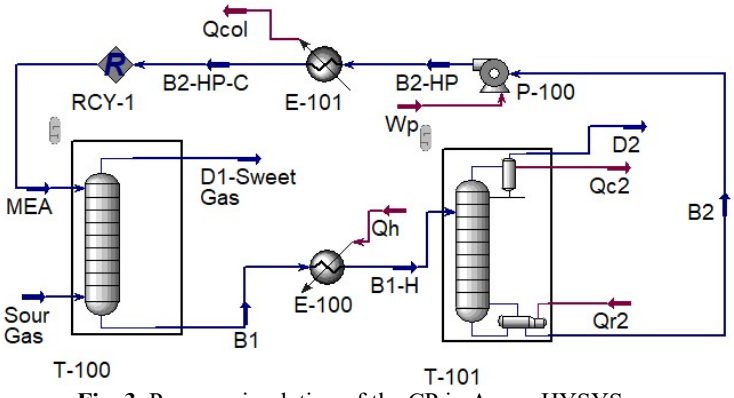

Fig. 3. Process simulation of the CP in Aspen HYSYS

Table 2. CP simulation specifications

	Absorption column	Solvent recovery column

Total stage		20	20
Feed stage	**MEA**	1	5
	Sour Gas	20	
Column top pressure [kPa]		4800	101.3
Column pressure drop [kPa]		100	28.7

4.2. Heat-integrated process (HIP)

In the first step, the process design aims to decrease the need for hot and cold utilities outside the columns by heat integration between the process flows. The bottom products of the absorption and recovery columns require hot and cold utilities, respectively, to reach the proper temperature conditions. Therefore, either of these two utilities can be eliminated completely and the other one can be reduced by exchanging heat between these two flows within a heat exchanger.

This process is depicted in Fig. 4. The heater for the absorption column is eliminated completely and the bottom product of the absorption column reaches 100˚C by absorbing heat from the bottom product of the solvent recovery column in a heat exchanger. Since the bottom product of the recovery column leaves the heat exchanger at 83.86˚C, a cold utility, as minimal level, is however, required to decrease the temperature to 30˚C. Therefore, by doing this, heater is removed completely and the required cold utility for the cooler is significantly reduced.

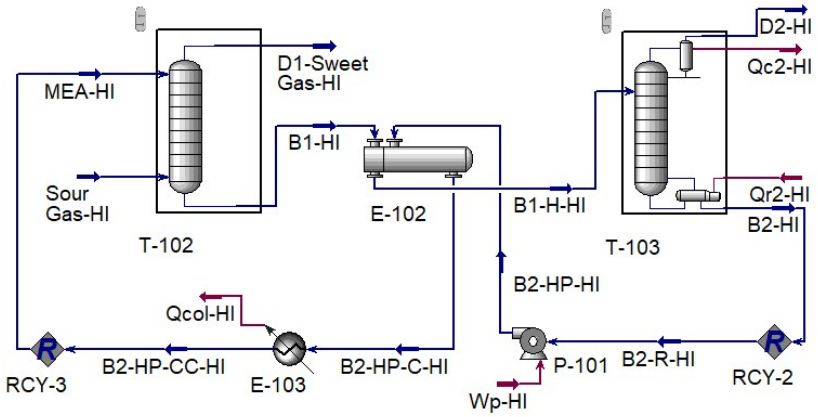

Fig. 4. Process simulation of the HIP in Aspen HYSYS

4.3. VRC method

In this process, the need for cold and hot utilities in the solvent recovery column of the HIP is reduced by the use of VRC. Based on Fig. 5, the outlet vapor at the top of the solvent recovery column is compressed to 165kPa upon passing the compressor.

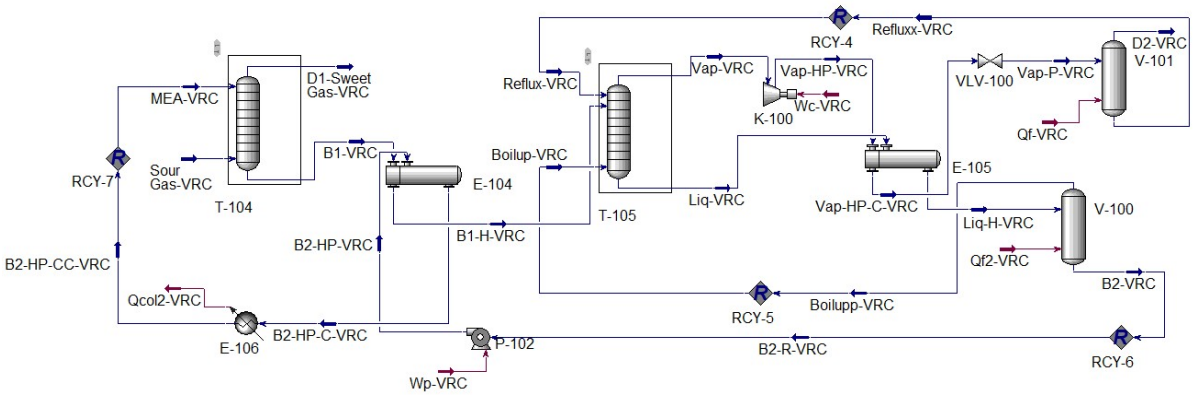

Fig. 5. Process simulation of the VRC method in Aspen HYSYS

Therefore, top vapor of the column reaches temperatures higher than the bottom liquid of the column, and heat can be transferred between the flows within a heat exchanger. The minimum allowable temperature difference of the heat exchanger is assumed 5˚C (ΔT^{app}_{min}=5). The cooled outlet fluid of the exchanger first passes the throttling valve to reach the top product pressure, and then enters the flash drum. The separated vapor and liquid phases serve as the top product and the reflux stream of the recovery column, respectively.

The heated outlet fluid of the heat exchanger also enters another separator; accordingly, the separated vapor phase supplies the boil-up stream of the recovery column and the separated liquid phase acts as the bottom product of the column. This product has the same composition of the initial solvent and returns to the absorption column after its pressure and temperature reach the initial solvent feed conditions. The separators added to the top and bottom products of the recovery column still require cold and hot utilities, whose values indicate a drastic decrease compared to the HIP process.

4.4. BF method

In this process, the need for the cold and hot utilities in the solvent recovery column in the HIP is resolved and declined by the use of BF approach. This process simulation is proposed in Fig. 6. Bottom outlet liquid of the recovery column, at first, passes through the throttling valve to reach the pressure of 77kPa. Therefore, the temperature of bottom liquid of the column fell below its top vapor and the top vapor can lose its heat to the bottom liquid within a heat exchanger. The minimum allowable temperature difference of the heat exchanger was taken 5˚C (ΔT^{app}_{min}=5). Since the heated outlet fluid of the exchanger is a two-phase fluid, a flash drum is needed to separate its phases as the first step. The separated phases, vapor and liquid flows, respectively pass through the pump and the compressor to reach their previous pressure and then they are combined as a mixed flow. Then, the mixed flow enters another separator to create the bottom product and the boil-up streams. Similarly, the outlet cooled fluid of the exchanger enters other two-phase separator to form the top product and the reflux streams of the recovery column.

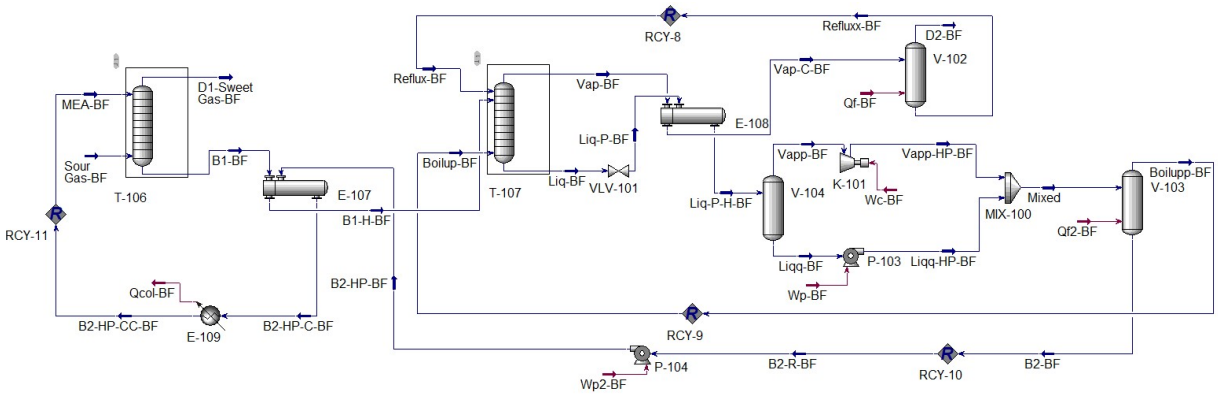

Fig. 6. Process simulation of the BF method in Aspen HYSYS

4.5. Total energy consumption

The energy consumption of the cold and hot utilities along with the required power of the compressor for each process is presented in Table 3. Fig. 7 also compares the total energy consumption of the four studied processes.

Table 3. Breakdown of energy consumption (compressor, cold, and hot utilities) for each studied process

Process	Hot utility (MW)	Cold utility (MW)	Compressor consumption (MW)
CP	80093	80098.7	---
HIP	49070	49065.6	---
VRC	2691	5311.7	**2354**
BF	1429	3936.7	**2545**

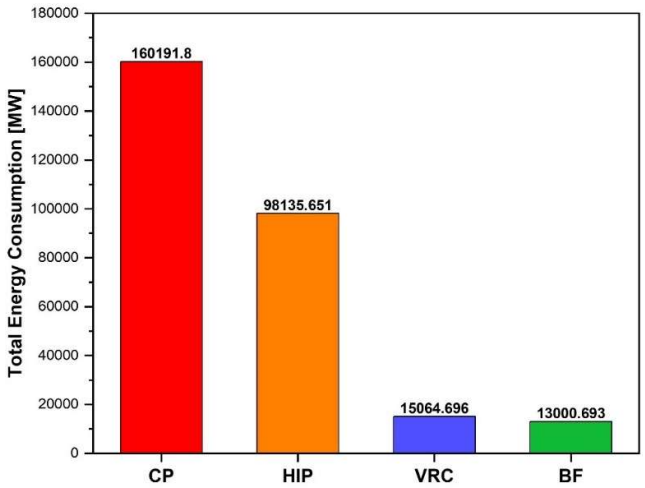

Fig. 7. Comparison of total energy consumption among the processes

Based on Fig. 7, all HIP, VRC, and BF managed to reduce total energy consumption of CP process. BF offered the highest energy saving; thus, BF was known as the optimum process. This result can be chiefly attributed to the drastic reduction in hot and cold utility consumption.

4.6. TAC

Table 4 investigates the number of required equipment in the four studied processes. The reboiler, heater, condenser, and cooler were considered as the heat exchanger equipment. Regarding the decline in the energy consumption in the VRC and BF methods and the increase in the number of the equipment and capital costs, TACs for the four mentioned processes were calculated to find the best process with the lowest TAC. The payback factor has been assumed as five years to annualize the capital investment. Moreover, cost index is obtained based on the chemical engineering plant cost index journal for 2022 (CE=622.5) to correlate capital costs according to Seider et al. [33].

Table 4. Number of required different equipment in the studied processes

Process	Heat exchanger	Distillation column	Separator	Pump	Compressor
CP	4	2	0	1	0
HIP	4	2	0	1	0
VRC	5	2	2	1	1
BF	5	2	3	2	1

The calculation results of TAC indicate that although BF employs the highest number of equipment, however, it can offer the highest reduce in the TAC of the CP. In Fig. 8, the TAC decrease percentage compared to the CP is reported for the HIP, VRC, and BF.

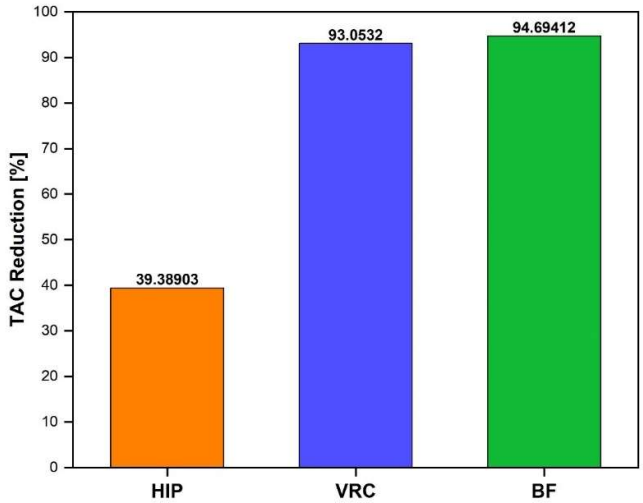

Fig. 8. Percentage reduction of the studied processes in TAC relative to the CP

As the energy consumption was remarkably lowered in the BF and VRC methods, compared to the CP, the decline in the TAC of these processes was also significant. Moreover, the lower energy consumption of BF compared to the VRC resulted in higher decline of TAC in the BF method compared to the others. Therefore, the BF method can be recognized as the optimal process in terms of TAC.

4.7. Exergy analysis

In this section, the exergy loss calculations were first carried out for each equipment of the four mentioned processes at 25˚C and 1 atm. Then the exergy efficiency (%) was determined for the heat exchangers, pumps, and compressors.

Table 5 presents the exergy loss of each equipment for different processes; while the exergy efficiency of pump, compressor, and heat exchanger are listed in Table 6.

Table 5. Exergy loss distribution [kW] across key equipment in the studied processes, in this table separator1 refers to V-100 in VRC and V-103 in BF, separator2 refers to V-101 in VRC and V-102 in BF, separator3 refers to V-104 in BF, heat exchanger1 refers to common heat exchanger in HIP, VRC, and BF, heat exchanger2 refers to E-105 in VRC and E-108 in BF, pump1 refers to common pumps in all processes, and pump2 refers to the added pump in BF

Item	Absorption column	Recovery column	Separator1	Separator2	Separator3	Heater	Cooler	Heat exchanger1	Heat exchanger2	Pump1	Pump2	Compressor	Throttling valve
CP	-9.64e+3	1.41e+7	-	-	-	90.0399	1.02e+3	-	-	35.06	-	-	1.41e+7
HIP	-8.30e+2	6.60e+6	-	-	-	-	4.56e+2	79.57	-	35.10	-	-	6.60e+6
VRC	-8.37e+2	1.01e+6	8.08e+3	1.34e+6	-	-	4.63e+2	78.13	6.94e+5	23.68	-	2.35e+6	5.43e+6
BF	-8.36e+2	1.01e+6	3.06e+3	2.39e+5	4.79e+4	-	4.62e+2	78.36	6.86e+5	23.68	35.02	2.54e+6	4.56e+6

Total exergy analysis of the four processes was conducted and the processes were compared in terms of total exergy loss and exergy efficiency. The system range was defined in such a way that the sour gas served as the input flow, while the sweet gas (distillate product of the absorption column) and distillate product of the recovery column were considered as the outflows.

Table 6. Exergy efficiency (%) of heat exchangers, pumps, and compressors in the studied processes, in this table heat exchanger 1 refers to common heat exchanger in HIP, VRC, and BF, heat exchanger 2 refers to E-105 in VRC and E-108 in BF, pump 1 refers to common pumps in all processes, and pump 2 refers to the added pump in BF

Item	Heat Exchanger 1	Heat Exchanger 2	Pump 1	Pump 2	Compressor
CP	-	-	81.37	-	-
HIP	82.56	-	81.35	-	-
VRC	82.63	86	80.34	-	82.6
BF	82.6	84.94	80.34	81.38	82.48

Furthermore, the heat flux of reboiler and heater were taken as the input flux; whereas heat fluxes of the condenser and cooler were regarded as the output heat flux. The power consumption of the pump and compressor were taken as the input work in the exergy analysis. According to Fig. 9 and 10, the BF method as the optimal process managed to minimize the total exergy loss to 2.5GW and maximize the total exergy efficiency to 0.43%.

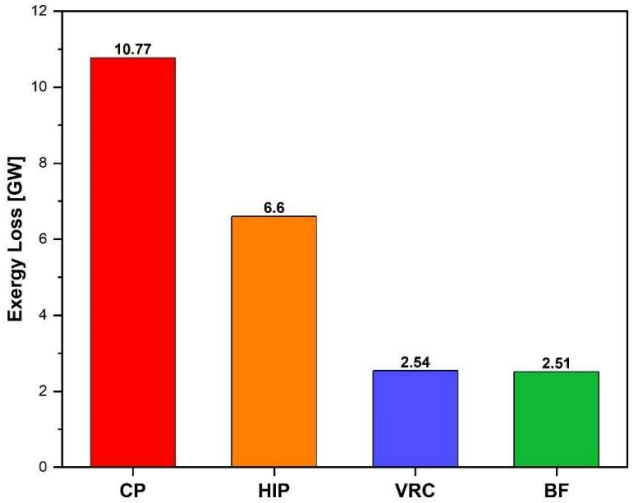

Fig. 9. Comparison of the total exergy loss in the four processes

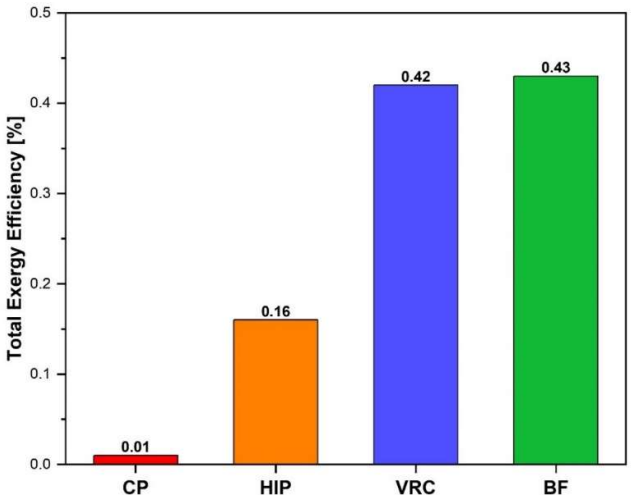

Fig. 10. Comparison of overall exergy efficiency (%) across the four processes

4.8. Environmental evaluation

In this final section, environmental assessments for all processes are presented, focusing on CO_2 emission rates. Given that the outlet stream temperatures from all reboilers or heaters equipped in the processes are approximately 111°C, LPS is deemed an appropriate heat utility. Therefore, the values for λ_{Proc} and h_{Proc} in the calculations are considered for LPS. As indicated in Fig. 11, BF and VRC could reduce the CO_2 emission of the CP by about 96 and 95%, respectively.

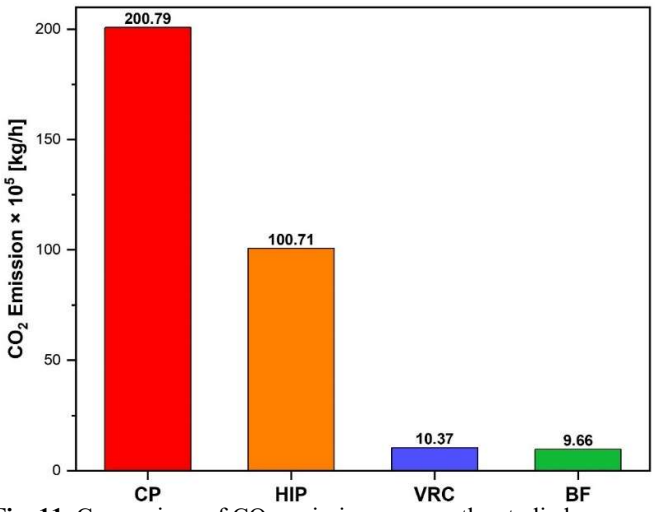

Fig. 11. Comparison of CO_2 emissions among the studied processes

4.9. Summary of key findings

Table 7 provides a concise summary of the key findings, emphasizing the advantages of the BF method over the VRC method based on the results discussed in previous sections.

Table 7. Comparison of BF and VRC methods based on key findings

Parameter	BF Method	VRC Method	Advantage of BF
Energy Consumption	92% reduction vs. CP	89% reduction vs. CP	Lower energy demand
Equipment Requirements	Requires one additional separator and pump compared to VRC	Requires one fewer separator and pump compared to BF	No advantage
TAC	95% reduction vs. CP	93% reduction vs. CP	More cost-effective
Exergy Efficiency	0.43%	0.39%	Higher efficiency
Exergy Loss	77% reduction vs. CP	75% reduction vs. CP	Lower exergy loss
CO_2 Emissions	96% reduction vs. CP	95% reduction vs. CP	More environmentally friendly

5. Conclusion

Natural gas sweetening by amine is a common process in the gas refineries to remove H_2S and CO_2. Nevertheless, this process is energy-intensive due to the presence of two extra columns and their heat demand which consequently makes the process unfriendly for the environment. Therefore, energy optimization of this process is highly required. The use of an efficient heat integration method can decline the utility consumption rate and process costs in addition to enhancing the environmental compatibility of the process.

In this research, VRC and BF methods were employed for heat integration of the gas sweetening process by amine solvent. These two methods were compared with two conventional approaches in gas refineries to determine their efficiency. To this end, four different processes were rigorously simulated in Aspen HYSYS V.11 software to compare their energy consumption, TAC, exergy loss, exergy efficiency, and CO_2 emissions. According to the results, both VRC and BF methods significantly decreased the TAC, exergy loss, and CO_2 emission rates of the process as well as increased the energy saving and exergy efficiency. Since the base process exhibits extremely low exergy

efficiency due to its high energy consumption, even a moderate improvement in exergy efficiency through heat integration is valuable.

The BF method exhibited better performance as it declined the energy consumption, TAC, exergy loss, and CO_2 emission by 92, 95, 77, and 96%, respectively; while raising the exergy efficiency from 0.01 to 0.43%. This improvement can be chiefly assigned to the elimination of hot and cold utilities in the amine recovery column. Although heat integration strategies significantly reduce energy consumption, complete elimination is not achieved, which limits the extent of exergy efficiency improvement. The VRC method also eliminated the need for the hot and cold utilities in the amine recovery column; however, its total energy consumption was about 14% higher than that of BF.

Overall, the BF approach proved to be the most economically and environmentally favorable method. Further reduction in energy consumption could lead to a substantial increase in exergy efficiency, enhancing the overall sustainability of the process.

Nomenclature

Acronyms		$\bar{G}$	Gibbs free energy per mole (kW)
BF	Bottom flashing	H	Enthalpy (kW)
HI	Heat integration	H_0	Enthalpy at environmental conditions (kW)
HIDiC	Internally heat-integrated distillation column	H_{mixing}	The heat of dissolution or mixing (kW)
LASSF	Lean amine stream Split flow	h_{Proc}	Enthalpy of stream (kJ/kg)
LPS	Low pressure steam	HIP	Heat-integrated process of natural gas sweetening
MDEA	Mono-diethanolamine	I	Exergy loss (kW)
MEA	Mono-ethanolamine	NHV	Net heating value (kJ/kg)
MPS	Medium pressure steam	Q	Total energy consumption (MW)
MVRHP	Mechanical vapor recompression heat pump	Q'	Total energy consumption (with compressor) (MW)
PPM	Proportion per million	Q_c	Condenser heat duty (MW)
RASSF	Rich-amine stream split flow	Q_{Fuel}	Fuel energy required for steam generation (kJ/h)
TAC	Total annual cost	Q_r	Reboiler heat duty (MW)
VRC	Vapor recompression	S	Entropy ($kW.K^{-1}$)
Symbols		S_0	Entropy at environmental conditions ($kW.K^{-1}$)
C%	Carbon content in fuel	T_0	Ambient temperature (K)
CP	Conventional process of natural gas sweetening	T_{FTB}	Flame temperature (˚C)
EX	Exergy (kW)	T_{Stack}	Stack temperature (˚C)
EX_{ch}	Chemical exergy (kW)	W_{comp}	Compressor duty (MW)
EX_k	Kinetic exergy (kW)	α	CO_2 molar mass ratio
EX_p	Potential exergy (kW)	λ_{Proc}	Latent heat of steam (kJ/kg)
EX_{ph}	Physical exergy (kW)	μ_i	Chemical potential of component I (kW)
EX_Q	Heat flux exergy (kW)	μ_{mix}	Chemical potential of mixture (kW)
EX_{stream}	Stream exergy (kW)	η	Exergy efficiency (%)
EX_W	Work exergy (kW)	ΔT^{app}_{min}	Minimum allowable temperature difference in heat exchanger (˚C)

References

[1] Paraschiv, S., Paraschiv, L.S., 2020. Trends of carbon dioxide (CO2) emissions from fossil fuels combustion (coal, gas and oil) in the EU member states from 1960 to 2018. Energy Reports, 6, 237-242. https://doi.org/10.1016/j.egyr.2020.11.116

[2] Burgers, W., Northrop, P., Kheshgi, H., Valencia, J., 2011. Worldwide development potential for sour gas. Energy Procedia, 4, 2178-2184. https://doi.org/10.1016/j.egypro.2011.02.104

[3] Chen, Z., Yang, G., Hao, X., Samak, N.A., Jia, Y., Peh, S., et al., 2021. Recent advances in microbial capture of hydrogen sulfide from sour gas via sulfur-oxidizing bacteria. Engineering in Life Sciences, 21(10), 693-708. https://doi.org/10.1002/elsc.202100006
[4] Abd, A.A., Naji, S.Z., Barifcani, A., 2020. Comprehensive evaluation and sensitivity analysis of regeneration energy for acid gas removal plant using single and activated-methyl diethanolamine solvents. Chinese Journal of Chemical Engineering, 28(6), 1684-1693. https://doi.org/10.1016/j.cjche.2019.12.004
[5] Rahmanpour, O., Zargari, M., Ghayyem, M., 2015. Application of artificial neural networks (ANNs) to Predict the rich amine concentration in gas sweetening processing units. Energy Sources, Part A: Recovery, Utilization, and Environmental Effects, 37(2), 118-126. https://doi.org/10.1080/15567036.2011.578111
[6] Qayyum, A., Ali, U., Ramzan, N., 2020. Acid gas removal techniques for syngas, natural gas, and biogas clean up–a review. Energy Sources, Part A: Recovery, Utilization, and Environmental Effects, 1-24. https://doi.org/10.1080/15567036.2020.1800866
[7] Song, C., Liu, Q., Ji, N., Deng, S., Zhao, J., Kitamura, Y., 2017. Natural gas purification by heat pump assisted MEA absorption process. Applied Energy, 204, 353-361. https://doi.org/10.1016/j.apenergy.2017.07.052
[8] Avor, E.P., Supap, T., Narku-Tetteh, J., Muchan, P., Natewong, P., Appiah, F.A., et al., 2023. Achieving net-zero CO2 emissions from indirect co-combustion of biomass and natural gas with carbon capture using a novel amine blend. International Journal of Greenhouse Gas Control, 130, 104005. https://doi.org/10.1016/j.ijggc.2023.104005
[9] Sibhat, M., Zhu, Q., Tsegay, G., Yao, G., Yin, G., Zhou, Y., et al., 2024. Enhancement technologies of ammonia-based carbon capture: A review of developments and challenges. International Journal of Greenhouse Gas Control, 136, 104196. https://doi.org/10.1016/j.ijggc.2024.104196
[10] Mohamadi-Baghmolaei, M., Hajizadeh, A., Zahedizadeh, P., Azin, R., Zendehboudi, S., 2021. Evaluation of hybridized performance of amine scrubbing plant based on exergy, energy, environmental, and economic prospects: A gas sweetening plant case study. Energy, 214, 118715. https://doi.org/10.1016/j.energy.2020.118715
[11] Pudi, A., Rezaei, M., Signorini, V., Andersson, M.P., Baschetti, M.G., Mansouri, S.S., 2022. Hydrogen sulfide capture and removal technologies: A comprehensive review of recent developments and emerging trends. Separation and Purification Technology, 298, 121448. https://doi.org/10.1016/j.seppur.2022.121448
[12] Einbu, A., Pettersen, T., Morud, J., Tobiesen, A., Jayarathna, C., Skagestad, R., et al., 2022. Energy assessments of onboard CO2 capture from ship engines by MEA-based post combustion capture system with flue gas heat integration. International Journal of Greenhouse Gas Control, 113, 103526. https://doi.org/10.1016/j.ijggc.2021.103526
[13] Muchan, P., Saiwan, C., Narku-Tetteh, J., Idem, R., Supap, T., Tontiwachwuthikul, P., 2017. Screening tests of aqueous alkanolamine solutions based on primary, secondary, and tertiary structure for blended aqueous amine solution selection in post combustion CO2 capture. Chemical Engineering Science, 170, 574-582. https://doi.org/10.1016/j.ces.2017.02.031
[14] Ellaf, A., Taqvi, S.A.A., Zaeem, D., Siddiqui, F.U.H., Kazmi, B., Idris, A., et al., 2023. Energy, exergy, economic, environment, exergo-environment based assessment of amine-based hybrid solvents for natural gas sweetening. Chemosphere, 313, 137426. https://doi.org/10.1016/j.chemosphere.2022.137426
[15] 1980. Energy conservation in distillation: a technology applications manual, Radian Corp., Austin, TX (United States), United States, (DOE/CS/4431-T2), Medium: ED; Size: Pages: 54. https://doi.org/10.2172/5159289
[16] Gai, H., Chen, S., Lin, K., Zhang, X., Wang, C., Xiao, M., et al., 2020. Conceptual design of energy-saving stripping process for industrial sour water. Chinese Journal of Chemical Engineering, 28(5), 1277-1284. https://doi.org/10.1016/j.cjche.2019.12.020
[17] Dai, Y., Peng, Y., Qiu, Y., Liu, H., 2019. Techno-economic analysis of a novel two-stage flashing process for acid gas removal from natural gas. Energies, 12(21), 4213. https://doi.org/10.3390/en12214213
[18] Long, N.V.D., Lee, M., 2017. Novel acid gas removal process based on self-heat recuperation technology. International Journal of Greenhouse Gas Control, 64, 34-42. https://doi.org/10.1016/j.ijggc.2017.07.003
[19] Al-Amri, A., Zahid, U., 2020. Design modification of acid gas cleaning units for an enhanced performance in natural gas processing. Energy & Fuels, 34(2), 2545-2552. https://doi.org/10.1021/acs.energyfuels.9b03671
[20] Liu, G., Zhu, L., Cao, W., Liu, H., He, Y., 2021. New technique integrating hydrate-based gas separation and chemical absorption for the sweetening of natural gas with high H_2S and CO_2 contents. ACS omega, 6(40), 26180-26190. https://doi.org/10.1021/acsomega.1c03165
[21] Sahl, A.B., Ahmed, M., Konga, Z.Y., Sunarso, J., 2023. Techno-economic analyses of Sulfinol-based absorber-stripper configurations for improving the energy consumption of natural gas sweetening process. South African Journal of Chemical Engineering, 43(1), 91-103. https://doi.org/10.1016/j.sajce.2022.10.003
[22] Lian, L., Liu, W., Liu, S., Wang, H., Cheng, L., Jiang, Y., 2023. Retrofit of the acid gas sweetening process for the refinery based on exergy analysis method. Separation and Purification Technology, 315, 123629. https://doi.org/10.1016/j.seppur.2023.123629
[23] Zarezadeh, F., Vatani, A., Palizdar, A., Nargessi, Z., 2022. Simulation and optimization of sweetening and dehydration processes in the pretreatment unit of a mini-scale natural gas liquefaction plant. International Journal of Greenhouse Gas Control, 118, 103669. https://doi.org/10.1016/j.ijggc.2022.103669
[24] Zhang, Y., Hou, Z., Yao, D., Qiu, X., Zhang, H., Cui, P., et al., 2023. Energy, exergy, economic and environmental comprehensive analysis and multi-objective optimization of a sustainable zero liquid discharge integrated process for fixed-bed coal gasification wastewater. Chinese Journal of Chemical Engineering, 58, 341-354. https://doi.org/10.1016/j.cjche.2022.10.012

[25] Odejobi, O.J., Jisieike, C.F., Anozie, A.N., 2015. Simulation and exergy analysis of processes for CO2 capture and utilisation for methanol production. International Journal of Exergy, 17(4), 456-474. https://doi.org/10.1504/IJEX.2015.071560
[26] Atsonios, K., Panopoulos, K., Grammelis, P., Kakaras, E., 2016. Exergetic comparison of CO2 capture techniques from solid fossil fuel power plants. International Journal of Greenhouse Gas Control, 45, 106-117. https://doi.org/10.1016/j.ijggc.2015.12.022
[27] Feyzi, V., Beheshti, M., Kharaji, A.G., 2017. Exergy analysis: A CO2 removal plant using a-MDEA as the solvent. Energy, 118, 77-84. https://doi.org/10.1016/j.energy.2016.12.020
[28] Bahmani, M., Shariati, J., Rouzbahani, A.N., 2017. Simulation and optimization of an industrial gas condensate stabilization unit to modify LPG and NGL production with minimizing CO2 emission to the environment. Chinese Journal of Chemical Engineering, 25(3), 338-346. https://doi.org/10.1016/j.cjche.2016.07.006
[29] Zheng, S., Jiang, Y., Jia, S., Wu, Y., Cui, P., 2024. Effect of the presence of trace sulfur dioxide on piperazine-based amine absorbents for carbon dioxide capture. Chinese Journal of Chemical Engineering. https://doi.org/10.1016/j.cjche.2024.05.003
[30] Nie, K., Shang, R., Miao, F., Wang, L., Liu, Y., Jiao, W., 2024. An integrated technology for the absorption and utilization of CO2 in alkanolamine solution for the preparation of BaCO3 in a high gravity environment. Chinese Journal of Chemical Engineering. https://doi.org/10.1016/j.cjche.2024.04.012
[31] Ahmadi, S., Eyvazi-Abhari, N., Esperi, M., Asvadi, H., Kamkar, F.E., Rahbari, S., 2022. Comparison of Vapor Recompression and Bottom Flashing Methods in Energy Optimization of Natural Gas Sweetening Process. Journal of Gas Technology. JGT, 7(2). https://doi.org/20.1001.1/jgt.2023.560634.1009
[32] Babaie, O., Esfahany, M.N., 2020. Optimization and heat integration of hybrid R-HIDiC and pervaporation by combining GA and PSO algorithm in TAME synthesis. Separation and Purification Technology, 236, 116288. https://doi.org/10.1016/j.seppur.2019.116288
[33] Seider, W.D., Seader, J.D., Lewin, D.R., 2009. Product and Process Design Principles: Synthesis, Analysis and Evaluation John Wiley & Sons.
[34] Braimakis, K., Karellas, S., 2023. Exergy efficiency potential of dual-phase expansion trilateral and partial evaporation ORC with zeotropic mixtures. Energy, 262, 125475. https://doi.org/10.1016/j.energy.2022.125475
[35] Hu, Z., He, D., Zhao, H., 2023. Multi-objective optimization of energy distribution in steel enterprises considering both exergy efficiency and energy cost. Energy, 263, 125623. https://doi.org/10.1016/j.energy.2022.125623
[36] Yu, A., Ye, Q., Li, J., Li, X., Wang, Y., Rui, Q., 2023. Improving the economy and energy efficiency of separating n-propanol/water/tetrahydrofuran via triple-column pressure-swing distillation and azeotropic combining pressure-swing distillation. Separation and Purification Technology, 309, 123023. https://doi.org/10.1016/j.seppur.2022.123023
[37] Geng, X., Yan, P., Zhou, H., Li, H., Gao, X., 2023. Process synthesis and 4E evaluation of hybrid reactive distillation processes for the ethanol and tert-butanol recovery from wastewater. Renewable Energy, 205, 929-944. https://doi.org/10.1016/j.renene.2023.01.107
[38] Babaie, O., Esfahany, M.N., 2022. Combining game theory and evolutionary algorithms for optimizing hybrid RDWC–pervaporation–vapor permeation process equipped with solar heating system. Journal of Cleaner Production, 376, 134235. https://doi.org/10.1016/j.jclepro.2022.134235

Appendix A: Economic calculations

Total capital investment evaluations in this research was based on the study of Sieder et al. [33] correlations [33]. The details of different types of utilities and their costs are presented in Table (A.1) [32]. The capital investment of the heat exchanger in condensers and kettle reboilers were determined by Eqs. (A.1) and (A.2), respectively at the carbon steel tube length of 6 m and pressure of 689kPa. The external area of tube, A, can vary from 14 to 1000m^2. The cost index of all correlations was obtained from the chemical engineering plant cost index journal in 2022 (CE=622.5).

$$C_{cond} = (CE/622.5)\exp\left\{11.4185 - 0.9228\left[\ln(10.76A)\right] + 0.09681\left[\ln(10.76A)\right]^2\right\} \quad (A.1)$$

$$C_{reb} = (CE/622.5)\exp\left\{12.3310 - 0.8709\left[\ln(10.76A)\right] + 0.09005\left[\ln(10.76A)\right]^2\right\} \quad (A.2)$$

Concerning shell and tube heat exchangers (in the U shape), the external area of tube, A, varies from 14 to 1000m^2 as determined by Eq. (A.3) (minimum temperature approach is 5˚C). Both shell and tubes are made of carbon steel. The expense of heat exchanger in this type was calculated from Eq. (A.4):

$$A = \frac{Q}{UA\Delta T_{\min}} \quad (A.3)$$

$$C_{HE} = (CE/622.5)\exp\{11.5510 - 0.9186[\ln(10.7639A)] + 0.09790[\ln(10.7639A)]^2\} \quad (A.4)$$

For pressure values above 689kPa, a pressure factor was utilized as follows:

$$F_P = 0.9803 + 0.018\left(\frac{P}{689}\right) + 0.0017\left(\frac{P}{689}\right)^2 \quad (A.5)$$

$$P(kPa):\ 689 < P < 13000 \quad (A.6)$$

Based on the compressor power, two kinds of compressor can be employed: screw compressor for powers below 149kW (<149kW) and centrifugal compressor for powers above 149kW (>149kW) (see Eqs. (A.7) and (A.8) respectively):

$$C_{ScrewCompressor} = (CE/622.5)F_D F_M \exp\{8.2496 + 0.7243[\ln(1.341P_C)]\} \quad \text{,for } P_C < 149 \text{ kW} \quad (A.7)$$

$$C_{CentrefugalCompressor} = (CE/622.5)F_D F_M \exp\{9.1553 + 0.63[\ln(1.341P_C)]\} \quad \text{,for } P_C > 149 \text{ kW} \quad (A.8)$$

F_D, a gas turbine drive, and F_M, stainless still material, were assumed 1.25 and 2.5, respectively. Eqs. (A.9) and (A.10) were employed to determine pump cost considering simplest type of cast iron.

$$S = Q(H)^{0.5} \quad (A.9)$$

$$C_B = (CE/622.5)exp\{12.1656 - 1.1448[\ln(S)] + 0.0862[\ln(S)]^2\} \quad (A.10)$$

The expense of vessel in vertical columns was determined based on its weight (W) in Eqs. (A.11-A.12). D_i is the vessel inside diameter [m], L is the tower height [m], and P_d is the column design pressure [kPa]:

$$C_V = (CE/622.5)\exp\left\{10.5449 - 0.4672\left[\ln(W)\right] + 0.05482\left[\ln(W)\right]^2\right\} \quad (A.11)$$

$$W = \pi\left(D_i \times 39.37 + \frac{P_d \times D_i}{593 - 0.03P_d}\right)(L \times 39.37 + D_i \times 31.5)0.284 \times \frac{P_d \times D_i}{2088 - 0.1P_d} \quad (A.12)$$

$$P_d = \exp\left\{0.60608 + 0.91615\left[\ln(P \times 0.145)\right] + 0.0015655\left[\ln(P \times 0.145)\right]^2\right\} \quad (A.13)$$

Cost of carbon steel sieve trays were determined by Eqs. (A.14-A.16) in which C_{BT} indicates the base cost of tray, N_T stands for the number of trays and F_{NT} denotes the correction factor.

$$C_T = N_T \times F_{NT} \times C_{BT} \tag{A.14}$$

$$C_{BT} = \left(CE / 622.5\right) 468 \exp(0.486 \times D_i) \tag{A.15}$$

$$N_T \geq 20 \qquad F_{NT} = 1$$
$$N_T < 20 \qquad F_{NT} = \frac{2.25}{1.0414^{N_T}} \tag{A.16}$$

Table A.1. Specifications of different types of utilities and electricity cost [32]

Utility	**Temperature [˚C]**	**Cost [USD.GJ^{-1}]**
LPS	160	13.28
Medium Pressure Steam (MPS)	184	14.19
High Pressure Steam (HPS)	254	17.7
Cooling Water	25	0.354
Electricity [USD.kW^{-1}.hr^{-1}]		0.07